ELSEVIER

Materials Science and Engineering A 415 (2006) 140–144

MATERIALS SCIENCE & ENGINEERING A

www.elsevier.com/locate/msea

# Effects of nitrogen ion implantation and implantation energy on surface properties and adhesion strength of TiN films deposited on aluminum by magnetron sputtering

Youming Liu [a,c], Liuhe Li [a,b], Ming Xu [a], Xun Cai [a], Qiulong Chen [a], Yawei Hu [a], Paul K. Chu [c,*]

[a] *School of Materials Science and Engineering, Shanghai Jiao Tong University, Shanghai 200030, China*
[b] *702 Department, Mechanical Engineering School, Beijing University of Aeronautic and Astronautic, Beijing 100083, China*
[c] *Department of Physics & Materials Science, City University of Hong Kong, Tat Chee Avenue, Kowloon, Hong Kong*

Received in revised form 31 August 2005; accepted 7 September 2005

**Abstract**

The performance of tribological coatings depends greatly on the adhesion strength between the coatings and substrates. In this work, we investigated the influence of the ion implantation energy of nitrogen on the adhesion and surface properties of TiN deposited on aluminum substrate. Aluminum samples were implanted with 15 keV, 30 keV and 40 keV nitrogen ions before TiN films were deposited using magnetron sputtering in a custom-designed multi-functional ion implanter. The adhesion properties of the implanted TiN films were assessed using nano-scratch tests and were observed to vary with the nitrogen ion implantation energy. Our frictional test results show that an appropriate ion implantation energy and dose can improve the frictional behavior of TiN films deposited on aluminum.
© 2005 Elsevier B.V. All rights reserved.

*Keywords:* TiN films; Nitrogen ion implantation; Adhesion strength; Frictional behavior

## 1. Introduction

Because of the light weight as well as high shearing strength, corrosion resistance, electrical conductivity and heat conductivity, aluminum alloys are widely used in the aerospace, electronic and automobile industries [1,2]. However, the low hardness and wear resistance of aluminum and aluminum alloys have hampered a wider application of the materials, particularly as load-bearing components and friction parts. Hence, it is necessary to improve the surface properties of the materials. Nitrogen ion implantation has been proposed to be a viable surface treatment technique in this respect [3–6]. By means of ion implantation, an aluminum nitride (AlN) surface layer can be formed and previous studies have shown that the nanohardness and frictional properties of implanted aluminum can be improved. However, owing to the relatively small projected range of the implanted nitrogen, the surface layer thickness is quite thin, usually around 100 nm [4], and consequently, the materials exhibit poor wear and tear characteristics in load-bearing applications.

TiN possesses good wear and corrosion resistance and is commonly used as a hard coating in industrial components such as cutting tools. In the work described here, we aim at enhancing the surface properties of aluminum by introducing nitrogen ion implantation prior to the deposition of TiN. This is contrary to the conventional practice in which a Ti interlayer is formed on the Al substrate before the TiN thin film is deposited. Nitrogen ion implantation is used here to generate a buffer layer between the TiN film and Al substrate to spread the stress gradually in order to enhance the resistance against a big load as well as plastic deformation. The effects of the nitrogen implantation energy on the adhesion strength, surface roughness and friction properties are also investigated.

## 2. Experimental details

Aluminum (99.99% pure) samples with dimensions of 15 mm × 15 mm × 5 mm were used in our experiments. The specimens were mechanically polished and ultrasonically cleaned in isopropyl alcohol for about 10 min prior to ion implantation. Ion implantation was conducted in a custom-designed multi-functional ion implanter equipped with a DC magnetron

* Corresponding author. Tel.: +852 27887724; fax: +852 27889549.
*E-mail address:* paul.chu@cityu.edu.hk (P.K. Chu).

0921-5093/$ – see front matter © 2005 Elsevier B.V. All rights reserved.
doi:10.1016/j.msea.2005.09.063

sputtering source, cathodic arc plasma source and Kaufman ion implantation source in the same vacuum chamber [7]. The samples were implanted with $N^+$ at energies of 15 keV, 30 keV, or 40 keV to a dose of $1 \times 10^{17}$ atoms/cm$^2$ or $2 \times 10^{17}$ atoms/cm$^2$. The ion beam current density was 25 $\mu$A/cm$^2$.

After ion implantation, the samples were rotated to face the magnetron sputtering target without breaking vacuum. The background pressure in the deposition chamber was less than $2 \times 10^{-3}$ Pa. The distance between the sample and sputtering target made of 99.4% pure Al was about 4–5 cm. The target voltage and current were 420 V and 1.0 A, respectively. The nitrogen and argon gases used in our experiments were 99.99% pure, and the total and $N_2$ partial pressure were $3.0 \times 10^{-1}$ Pa and $5.0 \times 10^{-2}$ Pa, respectively. A voltage of −60 V was applied to the samples during sputter deposition. The thickness of the deposited TiN layers was determined by profilometry to be about 1.7 $\mu$m.

The nano-scratch test apparatus was manufactured by CSEM Instruments. The tests were performed employing a Rockwell-shaped diamond indenter (50 $\mu$m radius) using a force, $F_N$, ranging from 0 N to 10 N applied to the samples in the normal direction. The samples were scratched by increasing the force at a rate of 7477.5 mN/min and a scratching speed of 6 mm/min over a distance of 8 mm. The friction and wear tests were performed utilizing a pin-on-disk tribometer. A $Si_3N_4$ ball with a diameter of 6 mm was used as the counterpart. The normal loading was 1 N, and the relative sliding speed was 220 mm/s. The tests were carried out under atmospheric pressure at a temperature of 25 °C and relative humidity of 50%.

The elemental depth profiles were determined by Auger electron spectrometry (AES) using a PHI 5500 ESCA/SAM. The primary electron energy was 3 keV and a 2 kV argon ion beam was used to obtain the depth profiles. Because the sputtered craters were quite shallow and the original surfaces were relatively rough, no depth measurements were performed. Instead, an average sputtering rate calculated from $SiO_2$ under similar sputtering conditions was used. The depths indicated in the AES depth profiles are thus approximate, but profile-to-profile comparison is valid. A VG Microlab MK-II instrument was used to acquire the X-ray photoelectron spectroscopy (XPS) spectra to study the chemical states of the elements in the implanted layer. A 5 kV $Ar^+$ beam was used to sputter the samples for 2 min to clean the surface before the XPS spectra were obtained. The Mg K$\alpha$ X-ray line was used as the excitation source.

## 3. Results and discussion

The O, Al, N depth profiles acquired from the 30 keV and 15 keV, $1 \times 10^{17}$ atoms/cm$^2$ samples prior to TiN deposition are displayed in Fig. 1. The N profiles exhibit a roughly Gaussian distribution and a high oxygen surface concentration is observed. The high-resolution Al 2p XPS spectrum shown in Fig. 2 indicates that the implanted layer consists of metallic aluminum (72.9 eV), AlN (73.9 eV) and aluminum oxide (74.9 eV) [4]. In previous reports [8,9], small carbon contamination was observed but it could not be detected in our samples to the AES detection limit.

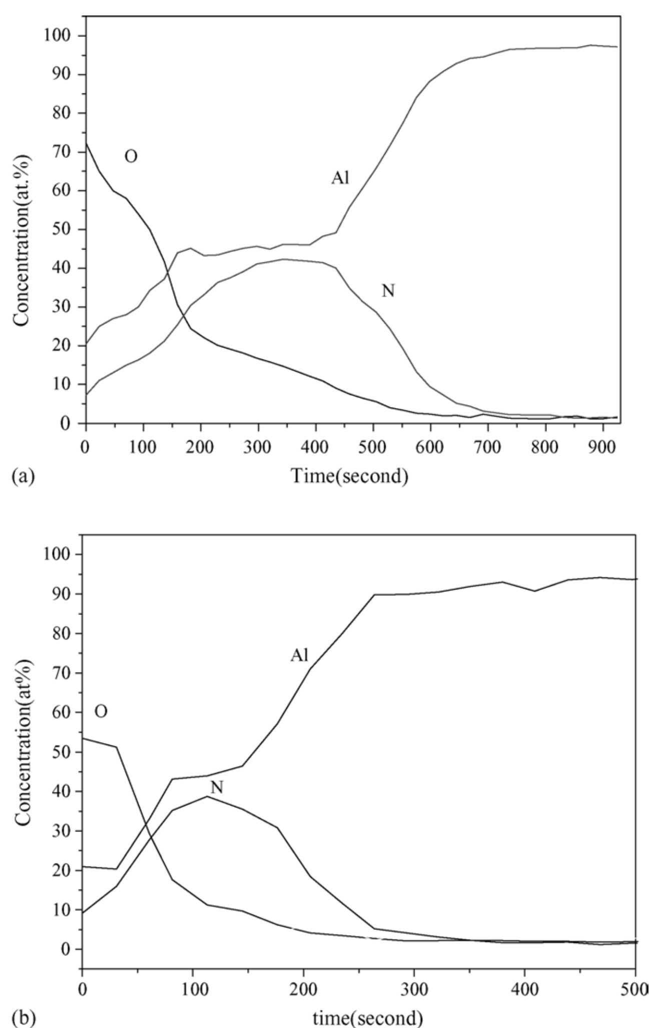


Fig. 1. Depth profiles of Al, Ti, O and C in the $N^+$-implanted aluminum: (a) 30 keV, $1 \times 10^{17}$ atoms/cm$^2$ and (b) 15 keV, $1 \times 10^{17}$ atoms/cm$^2$.

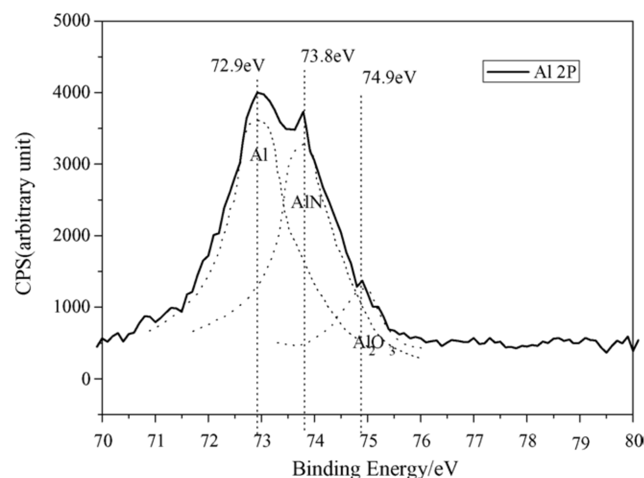


Fig. 2. High-resolution Al 2p XPS spectrum showing the three components with binding energies of Al (72.9 eV), AlN (73.8 eV) and $Al_2O_3$ (74.9 eV) acquired from the $N^+$-implanted sample (30 keV, $1 \times 10^{17}$ atoms/cm$^2$).

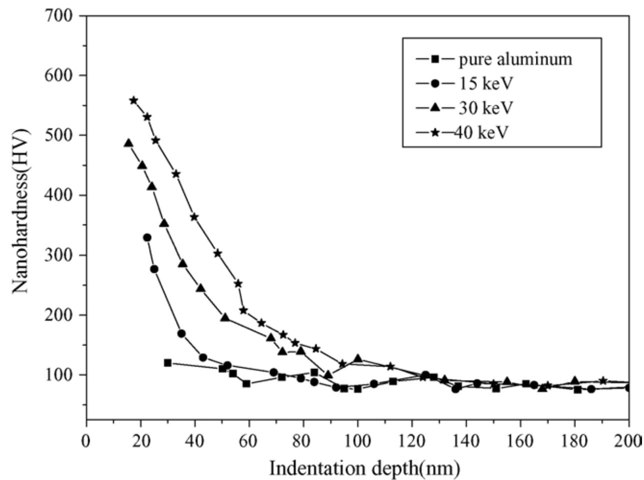


Fig. 3. Nanohardness of aluminum samples as a function of indentation depth.

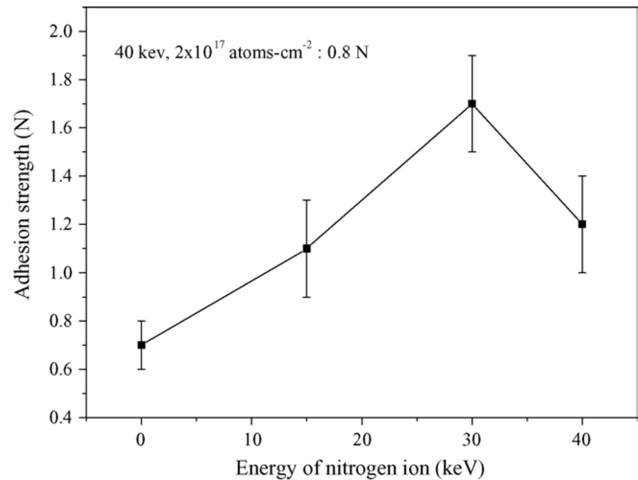


Fig. 4. Adhesive strength as a function of ion implantation energy.

The nanohardness values as a function of the indentation depth of the nitrogen-implanted and unimplanted aluminum samples are plotted in Fig. 3. A series of indentations were made to depths ranging from 20 nm to 200 nm depending on the loads. The compound hardness was calculated using the method proposed by Oliver and Pharr [10]. Each data point represents an average of five indentations. For the 40 keV sample, the hardness at 20 nm is 560 HV for an applied maximum load of 0.1 mN. The hardness decreases with increasing indentation depth in the near surface region and then reaches a constant value of 65 HV afterwards. In order to measure the "film-only" properties, a common rule of thumb is to limit the indentation depth to less than 10% of the thickness [10,11]. In this work, the thickness of the implanted layer is about 100 nm, and consequently, the indentation depth must be less than 10 nm. However, the minimum indentation depth of the implanted sample is 20 nm. Therefore, the hardness values combine the effects of the implanted layer and bulk substrate. An increase in hardness is expected but only at a smaller load. In this work, the loading ranges from 0.1 mN to 300 mN. The composite hardness decreases with smaller nitrogen ion implantation energy because of the shallower depth profiles. For the unimplanted sample, a compact amorphous $Al_2O_3$ layer typically 5 nm thick grows on Al when it is exposed to air [12,13]. Therefore, the hardness is almost constant throughout the indentation depth.

Fig. 4 shows the adhesion strength between the TiN films and aluminum substrates implanted with nitrogen at the same dose ($1 \times 10^{17}$ atoms/cm$^2$) but different energies. The adhesion strength is 0.7 N for the TiN film deposited on the untreated aluminum substrate. It increases to 1.7 N for the 30 keV sample but decreases to 1.2 N for the 40 keV sample. In comparison, the adhesion strength is only 0.8 N when the implantation energy and dose are 40 keV and $2 \times 10^{17}$ atoms/cm$^2$, respectively.

Fig. 5 shows the optical micrographs of the scratch channels on the various samples. The higher the dose and implantation energy, the coarser is the surface of the TiN film, especially when the ion implantation energy and dose reach 40 keV and $2 \times 10^{17}$ atoms/cm$^2$, respectively. Mitsuo et al. [14] reported the effects of the bias voltage on the temperature of steels during nitrogen plasma immersion ion implantation and observed that the substrate temperature rose to about 660 K at a bias voltage of 20 kV (RF power = 500 W, time = 3 h, maximum duty cycle = 20%). In our work, the nitrogen ions were generated in a Kaufman source. Since the implantation process was continuous and no sample cooling was conducted, the temperature of the substrate surface rose quickly. After implantation, the TiN film was immediately deposited using magnetron sputtering onto the "unoxidized" surface as vacuum was not broken. It has been reported that large crystallites, so-called hillocks, tend to outgrow above the initial surface of aluminum alloy films [15,16]. The driving force of hillock growth is a compressive stress caused by a large mismatch of thermal expansion coefficients between the film and substrate. Usually, hillocks tend to form in metal films. In our work, however, it is believed to be due to the effect of ion implantation into the aluminum substrate. With increasing ion energy and dose, the higher aluminum substrate temperature causes aluminum surface to recrystallize. The compressive stress generated during deposition of the TiN film causes some large crystallites outgrow above the surface of the aluminum substrate. The mechanism is the same as the formation of hillocks. Fig. 5(e) shows that the surface of the 40 keV, $1 \times 10^{17}$ atoms/cm$^2$ samples contain hillock-like islands. When the implant dose exceeds $2 \times 10^{17}$ atoms/cm$^2$, trenches appear on the surface of the sample as shown in Fig. 5(g). It is probably due to the merging of hillock-like islands or deformation of aluminum surface because of its soft properties and low melting point.

It can be observed in Fig. 5(a) that the bottom of the scratch channel is smooth, but slight buckling occurs at the edge of the scratch channel. It is known that aluminum undergoes large plastic deformation even when subjected to a small load (1 N). For a system comprising a hard surface film on a soft substrate, both the film and substrate give way to accommodate part of the indenter displacement. The stress concentrates in the edge of the scratch due to the difference in the properties between TiN and aluminum, and hence, the TiN film in this region tends to buckle and crack. With increasing loading, the interfacial cohesive stress increases, and the cracks ahead of the indenter propagate

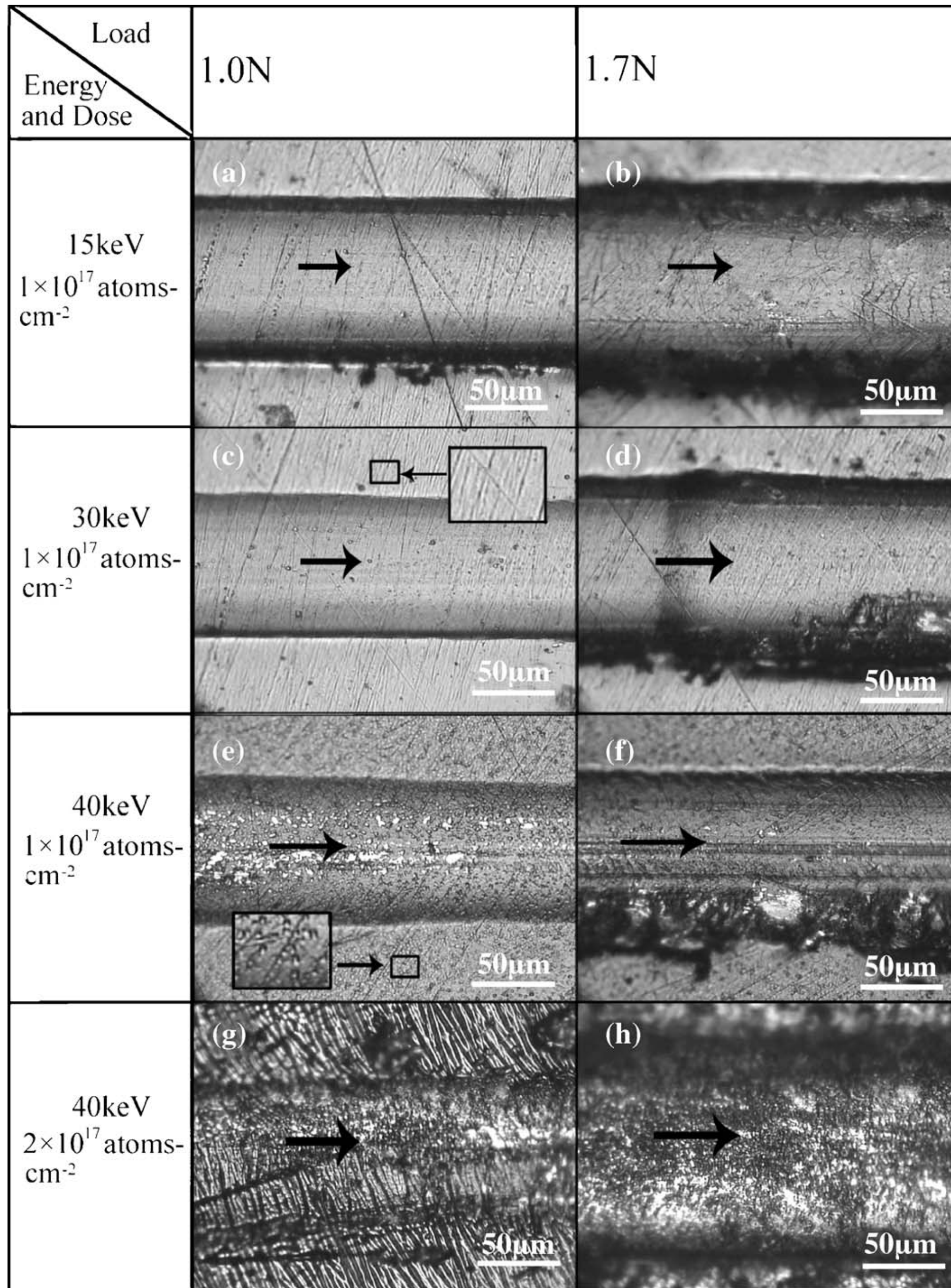


Fig. 5. (a–h) Micrographs of scratch channels. The arrows indicate the sliding direction.

to form semi-circular cracks. The schematic of failure mode is illustrated in Fig. 6. Fig. 5(c) does not show buckling at the edge of the scratch under a loading of 1 N and it can be attributed to the higher support capacity of the nitrogen-implanted layer and reduced stress concentration. Fig. 5(e and g) indicates partial spalling at the bottom of the scratch, because the humped defects are deformed under the indenter. When a larger load is applied, either the brittle nature of the coating or the stored elastic energy is sufficient to cause spallation and fracture at the edge and front of the indenter. Fig. 5(b, d, f and h) shows the micrographs of the scratch channels of the different samples under a loading of 1.7 N and spallation and cracking can be observed on all them to different extent.

Fig. 7 shows the effects of the nitrogen ion implantation energy on the kinematic friction behavior of the TiN film against a $Si_3N_4$ ball. The pure aluminum sample has a low friction coefficient of about 0.3 at the beginning of the measurement and then suddenly increases to a high value of approximately 1.2 after the dense $Al_2O_3$ film on the surface has been broken through. TiN also reduces the friction coefficient significantly. The friction coefficient of the TiN films on aluminum quickly rises from 0.28 to 0.73 for a distance of 0–40 m. After the aluminum sub-

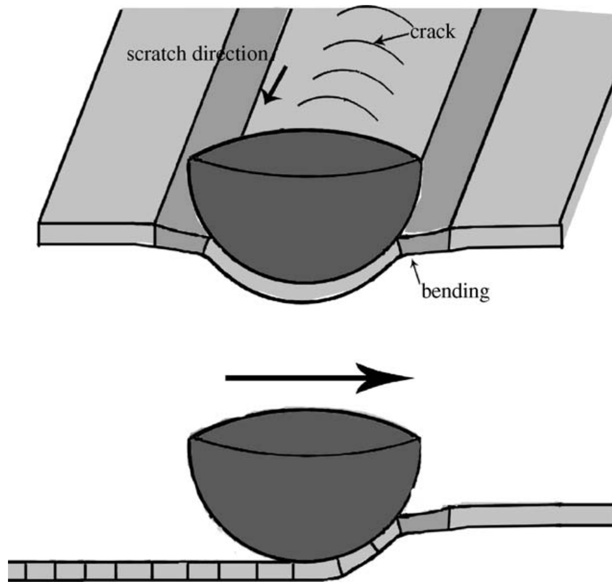


Fig. 6. Schematic of failure mode.

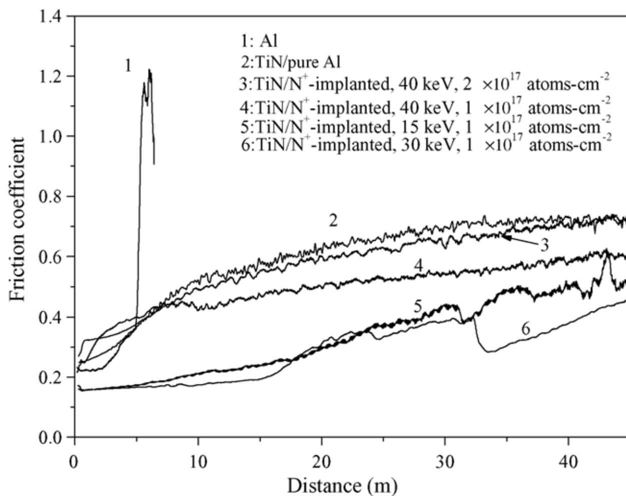


Fig. 7. Friction coefficients of pure aluminum and TiN films on different types of substrates.

strate has been implanted with 15 keV nitrogen ion to a dose of $1\times10^{17}$ atoms/cm$^2$, the friction coefficient gradually rises from 0.18 to 0.5 for a distance of 0–45 m. For the TiN film on aluminum that has been implanted with 30 keV, $1 \times 10^{17}$ atoms/cm$^2$ nitrogen, a slower increase in the friction coefficient is observed. In the two cases mentioned above, fluctuations are observed during the rising part of the friction coefficient curves. Spallation at the edge of the scratch channel depicted in Fig. 5(b and d) may be the cause of the fluctuations. For the same ion implantation dose, when the implantation energy is increased to 40 keV, the friction coefficient rises from 0.4 to 0.6 for 0–45 m. A higher friction coefficient is observed on the 40 keV, $2 \times 10^{17}$ atoms/cm$^2$ implanted sample. This phenomenon may be explained by the weak adhesion strength between the TiN films and the substrate.

## 4. Conclusion

Our results show that nitrogen ion implantation into aluminum prior to TiN deposition enhances the adhesion strength of the film and tribological properties. XPS results show that the implanted layer consists of Al, TiN and a surface oxide layer. The composite hardness of the nitrogen-implanted aluminum surface is increased. However, it diminishes with decreasing nitrogen ions energy because of shallower penetration of nitrogen. An appropriate ion energy and dose are found to improve the adhesion strength between the TiN film and aluminum substrate. The optimum implantation energy and dose determined experimentally are 30 keV and $1 \times 10^{17}$ atoms/cm$^2$, respectively. The same implantation energy and dose also yield the best frictional behavior.

## Acknowledgements

This work was supported by City University of Hong Kong Direct Allocation Grant 9360110 and National Natural Science Foundation of China No. 50271004.

## References

[1] E.A. Starke Jr., J.T. Staley, Prog. Aerospace Sci. 32 (1996) 131.
[2] P.K. Rohatgi, Fuel Energy Abstr. 39 (1998) 25.
[3] J. Jagielskia, A. Piatkowska, P. Aubert, C. Legrand-Buscema, Vacuum 70 (2003) 147.
[4] J. Chakraborty, S. Mukherjee, P.M. Raole, P.I. John, Mater. Sci. Eng. A 304–306 (2001) 910.
[5] H.K. Sanghera, J.L. Sullivan, S.O. Saied, Appl. Surf. Sci. 141 (1999) 57.
[6] B.W. Karr, I. Petrov, D.G. Cahill, J.E. Greene, Appl. Phys. Lett. 70 (1997) 1703.
[7] X. Cai, H.H. Tong, Q.C. Chen, S.H. Pu, J. Zhao, Q.L. Chen, Y.M. Liu, China Patent, CN 1,472,360.
[8] S. Mukherjee, F. Prokert, E. Richter, W. Möller, Thin Solid Films 445 (2003) 48.
[9] N. Dilawar, R. Kapil, Brahamprakash, V.D. Vankar, D.K. Avasthi, D. Kabiraj, G.K. Mehta, Thin Solid Films 323 (1998) 163.
[10] W.C. Oliver, G.M. Pharr, J. Mater. Res. 7 (1992) 1564.
[11] N.G. Chechenin, J. Bottiger, J.P. Kroge, Thin Solid Films 261 (1995) 219.
[12] R. Checchetto, L.M. Gratton, A. Miotello, Surf. Coat. Technol. 158–159 (2002) 356.
[13] L.H. Milacek, R.D. Daniels, J.A. Cooley, J. Appl. Phys. 39 (1968) 2803.
[14] A. Mitsuo, S. Uchida, T. Aizawa, Surf. Coat. Technol. 186 (2004) 196.
[15] F.Y. Génin, Acta Metal. Mater. 43 (1995) 4289.
[16] M. Zaborowski, P. Dumania, Microelectron. Eng. 50 (2000) 301.